Materials Science & Engineering C 118 (2021) 111519

Contents lists available at ScienceDirect

Materials Science & Engineering C

journal homepage: www.elsevier.com/locate/msec

Growth factor loaded *in situ* photocrosslinkable poly(3-hydroxybutyrate-*co*-3-hydroxyvalerate)/gelatin methacryloyl hybrid patch for diabetic wound healing

Robin Augustine[a,b], Anwarul Hasan[a,b,*], Yogesh B. Dalvi[c], Syed Raza Ur Rehman[a,b], Ruby Varghese[c], Raghunath Narayanan Unni[d], Huseyin C. Yalcin[b], Rashad Alfkey[e], Sabu Thomas[f], Ala-Eddin Al Moustafa[b,g]

[a] *Department of Mechanical and Industrial Engineering, College of Engineering, Qatar University, Doha 2713, Qatar*
[b] *Biomedical Research Center, Qatar University, Doha 2713, Qatar*
[c] *Pushpagiri Research Centre, Pushpagiri Institute of Medical Science & Research, Tiruvalla, Kerala 689101, India*
[d] *RP MedHelix Diagnostics Private Limited, Cochin, Kerala 682025, India*
[e] *Hamad Medical Corporation, Doha 3050, Qatar*
[f] *International and Inter University Center for Nanoscience and Nanotechnology, School of Chemical Sciences, Mahatma Gandhi University, Kottayam, Kerala 686560, India*
[g] *College of Medicine, QU Health, Qatar University, Doha 2713, Qatar*

ARTICLE INFO

Keywords:
GelMA
EGF
Electrospinning
Diabetic wound healing
Growth factor delivery

ABSTRACT

Management of chronic diabetic ulcers remains as a major challenge in healthcare which requires extensive multidisciplinary approaches to ensure wound protection, management of excess wound exudates and promoting healing. Developing wound healing patches that can act as a protective barrier and support healing is highly needed to manage chronic diabetic ulcers. In order to boost the wound healing potential of patch material, bioactive agents such as growth factors can be used. Porous membranes made of nanofibers generated using electrospinning have potential for application as wound coverage matrices. However, electrospun membranes produced from several biodegradable polymers are hydrophobic and cannot manage the excess exudates produced by chronic wounds. Gelatin-methacryloyl (GelMA) hydrogels absorb excess exudates and provide an optimal biological environment for the healing wound. Epidermal growth factor (EGF) promotes cell migration, angiogenesis and overall wound healing. Poly(3-hydroxybutyrate-*co*-3-hydroxyvalerate) (PHBV) membranes provide microbial, thermal and mechanical barrier properties to the wound healing patch. Herein, we developed a biodegradable polymeric patch based on the combination of mechanically stable electrospun PHBV, GelMA hydrogel and EGF for promoting diabetic wound healing. *In vitro* and *in vivo* studies were carried out to evaluate the effect of developed patches on cell proliferation, cell migration, angiogenesis and wound healing. Our results showed that EGF loaded patches can promote the migration and proliferation of multiple types of cells (keratinocytes, fibroblasts and endothelial cells) and enhance angiogenesis. *In situ* development of the patch and subsequent *in vivo* wound healing study in diabetic rats showed that EGF loaded patches provide rapid healing compared to control wounds. Interestingly, 100 ng EGF per cm^2 of the patches was enough to provide favourable cellular response, angiogenesis and rapid diabetic wound healing. Overall results indicate that EGF loaded PHBV-GelMA hybrid patch could be a promising approach to promote diabetic wound healing.

1. Introduction

Wound healing remains a major challenge in diabetic patients that results in morbidity and mortality due to several complications such as systemic inflammatory responses, severe sepsis and amputation of limbs [1]. Approximately 20% of all diabetic patients suffer from chronic ulcers at least once in their lifetime [2,3]. Co-occurrence of peripheral neuropathy and vascular diseases in diabetic patients increase the chances of ulceration due to loss of pain-sensation and peripheral ischemia [4–6]. Presence of significantly larger population of

* Corresponding author at: Department of Mechanical and Industrial Engineering, College of Engineering, Qatar University, Doha 2713, Qatar.
E-mail address: ahasan@qu.edu.qa (A. Hasan).

https://doi.org/10.1016/j.msec.2020.111519
Received 29 March 2020; Received in revised form 11 September 2020; Accepted 15 September 2020
Available online 18 September 2020

inflammatory cells which produce proteases like matrix metalloproteinases (MMPs) result in a shortage of growth factors that provide the cues for cell proliferation, migration, angiogenesis and wound healing [7]. Localized delivery of growth factors in diabetic ulcers offer great promise for optimal wound management as they activate various cellular responses such as cell migration, proliferation, and differentiation to facilitate rapid wound healing [8,9]. As a result of the excellent mitogenic effects on epithelial, fibroblastoid, and endothelial cells, epidermal growth factor (EGF) is used in clinics as a wound healing agent [10]. There are several reports on the topical application of EGF on cutaneous wounds for facilitating rapid wound healing [11,12]. Since the chronic wound microenvironment is hostile for local EGF bioavailability, administration of EGF in the diabetic wounds using a biopolymeric patch could be a promising approach to provide its long-term bioactivity.

In order to reduce the complications of diabetic wounds, wound healing patches with exudate uptake capacity, ability to prevent pathogenic invasion and wound healing properties should be applied over the wound [13,14]. The application of a suitable biodegradable patch could be a robust approach for protecting the wound and promoting wound healing. Several synthetic and natural polymers have been used for the development of degradable wound healing patches to manage chronic diabetic wounds [15–17]. Additionally, hydrogels attract increasing interest in wound healing applications since they can be applied directly on the wound which allows them to align perfectly with wound margins [6,18,19]. Hydrogels can hold a high water content and can thus absorb exudates at the wound site; this offers ideal conditions for skin hydration, healing, and removing necrotic tissue [20–23]. On the other hand, Gelatin-methacryloyl (GelMA) based wound healing patches are highly promising for wound healing applications due to their biocompatibility, biodegradability, low cost and simplicity of processing [24–28]. In addition, GelMA has received wide acceptance for the encapsulation and localized delivery of bioactive agents like growth factors [29–31]. However, the ability of GelMA to form a physical barrier over the wound for the entire duration of healing is limited due to its inferior mechanical strength and relatively fast degradation [32–34]. In order to ensure the complete success of wound healing patch during its entire period, a practical design that relies on multiple components is required. Incorporation of agents that can enhance healing will be necessary to achieve the desired outcome in chronic wound healing. Therefore, incorporation of bioactive agents such as EGF in GelMA component of the patch could be a good approach to improve the biological performance of the patch such as host cells proliferation, enhancement of cell migration to wounded area and enhanced angiogenesis at the application site [35,36].

Use of a secondary support material over the GelMA hydrogel layer with a relatively hydrophobic and mechanically stable polymer could be a promising strategy to protect the wound bed from pathogenic microorganisms and facilitate healing. Poly(3-hydroxybutyrate-*co*-3-hydroxyvalerate) (PHBV) can be a good candidate for this purpose because of its biocompatibility, biodegradability and mechanical strength [37]. PHBV is already explored in many biomaterial applications such as drug delivery systems, tissue engineering scaffolds and wound dressings [38]. An interesting study indicated that PHBV nanofiber meshes were able to promote wound healing and mitigate scar formation [39]. Although hydroxyvalerate content in PHBV can enhance the degradation and cell proliferation for some extent [40], this alone is not sufficient to make it a suitable biomaterial for wound healing applications [41]. Approaches like blending with other natural polymers [42], bioactive proteins [43], surface treatment [44], loading nanoparticles [45,46] are being tried to improve the wound healing performance of PHBV based wound dressings or patches.

Electrospinning technique can be used for the fabrication of highly porous membranes composed of fibers with submicrometer-diameter from a wide range of natural and synthetic polymers [47]. In addition to wound healing applications [48–51], electrospun membranes are used in several biomaterial applications such as drug delivery systems [8], tissue engineering scaffolds [52–57] and biomedical implants [58,59]. Electrospun membranes can effectively prevent the pathogenic colonization in wounds due to their microbial barrier property associated with closely packed fiber network [60]. Moreover electrospun fibers can act as cell guidance channels to facilitate the migration of neighboring host cells to the healing wound [45]. Thus, we herein report the development of EGF loaded wound healing patch based on GelMA hydrogel and PHBV meshes for diabetic wound healing applications. The developed patches were tested for cell proliferation and viability using fibroblasts and keratinocytes. *In vivo* studies in mice demonstrated that EGF loaded patches promoted cell proliferation, cell migration, angiogenesis and diabetic wound healing. Obtained results suggest that EGF-containing hybrid patches have remarkable potential for diabetic wound healing applications.

2. Experimental section

2.1. Fabrication of PHBV membranes

For electrospinning, 20% *w/v* PHBV (Mw = 6,80,000 $gmol^{-1}$, 12% PHV content, Sigma Aldrich) solutions were prepared in chloroform/DMF mixture (9:1). The prepared solution was taken in 10 mL syringe with an 18-gauge needle and electrospun at 15 cm tip to collector distance. A stationary steel plate was used as the collector. A flow rate of 2.5 $mL{\cdot}h^{-1}$ and 18 kV DC voltage were maintained during the electrospinning process. Obtained membranes were removed from the collector plate and used for the preliminary characterization and development of hybrid patches.

2.2. Development of EGF loaded hybrid patches

GelMA was synthesized as described in an earlier report [61]. Briefly, gelatin (Type A) was dissolved in PBS at 60 °C and 8 mL MA was added for every 100 mL of gelatin solution under vigorous stirring (50 °C) and the reaction was continued for 3 h. The reaction was stopped by adding excess preheated PBS (50 °C). The solution was then dialyzed and then freeze-dried to obtain GelMA. GelMA solutions were prepared by vortexing the required amount of GelMA to get 5% *w/v* solution in phosphate-buffered-saline (PBS, pH 7.4). All GelMA solutions contained a final concentration of 0.5% (*w/v*) 2-hydroxy-4′-(2-hydroxyethoxy)-2-methylpropiophenone (Irgacure 2959). Detailed information regarding the optimization studies of GelMA hydrogel preparation can be found in our earlier publication [17]. To produce bilayered patch, PHBV meshes were immersed in PBS for 1 h. Then, 200 μL GelMA solution was taken on a glass cover slip, wet PHBV membranes (2 × 2 cm) were kept over the GelMA droplet and gently pressed for 30 s to facilitate the infiltration of the solution into the pores of the membrane and obtain hybrid PHBV-GelMA patches. To get EGF loaded patches, four EGF concentrations were used, namely, 25 ng/cm^2, 50 ng/cm^2, 100 ng/cm^2 and 150 ng/cm^2 which were mixed with the GelMA solution just before infiltration in scaffolds. The GelMA in the hybrid patches was stabilized by UV crosslinking (Omnicure S2000, 10 s, 500 nm, 7 $mwWcm^{-2}$). Fabricated hybrid meshes were washed in ultrapure water for 5 min to remove unreacted reagents. Although we developed patches containing four different concentrations of EGF, based on the preliminary *in vitro* cell culture experiments (Supporting Information, Figs. S1–S3), hybrid patches containing 100 ng/cm^2 EGF (denoted as PHBV-GelMA-EGF) were only used for detailed analysis. In order to further verify the effective loading of EGF, we tested the loading of rhodamine conjugated bovine serum albumin as a model protein (Details are provided in supporting information, Fig. S4).

2.3. Physical characterization of the patches

The morphology of the developed PHBV meshes and hybrid patches

was investigated using a scanning electron microscope (SEM). Before the analysis, patches were dried in a hot air oven (40 °C) for 24 h, and then sputter coated with gold for a few minutes. Gold coated samples were analyzed using FEI, Nova NanoSEM, 450 FE-SEM at 10 kV. Average fiber diameter was obtained from the electron micrographs using ImageJ software. X-Ray Diffractometer (XRD, MiniFlex, Rigaku, Tokyo, Japan, 2θ range 0–60°, 40 KV voltage, 30 mA current) was used to determine the presence of GelMA coating on the meshes. Fourier transform infrared (FT-IR) analysis of PHBV meshes, GelMA and patches was performed with a Perkin Elmer Frontier MIR spectrophotometer with a PIKE Gladi ATR (USA) attachment at 4 cm^{-1} resolution in the range 4000–400 cm^{-1}.

2.4. Mechanical strength

The tensile properties of PHBV meshes, PHBV-GelMA patches and PHBV-GelMA-EGF patches were determined by uniaxial tensile tests of samples with a size of 6 × 1 cm^2 under a displacement rate of 1 mm/min. The thickness of the samples was 1.4 ± 0.2 mm. The Young's modulus of patches was defined as the slope of linear elastic region of the stress-strain curves.

2.5. Swelling characterization and determination of water contact angle

2.5.1. Swelling

Swelling study of the patches were performed to understand the exudate uptake capacity of the patches. Accurately weighed dry PHBV meshes and hybrid patches were soaked in PBS at 37 °C for different time intervals until fully hydrated and weighed again to get the wet weight of the samples. The swollen samples were then washed with distilled water (3 times), dried in a hot air oven (40 °C for 5 days), and reweighed. The swelling (%) was calculated by the Eq. (1).

$$\text{Swelling}\ (\%) = [(W^W - W^D)/W^D] \times 100 \quad (1)$$

where W^W and W^D are the wet and dry weight of the membranes respectively.

2.5.2. Water contact angle

Hydrophilicity of the patches were obtained from the water contact angle measurements (Phoenex-KGV-5000). A small water droplet was kept on the surface of PHBV, PHBV-GelMA or PHBV-GelMA-EGF samples (2 × 2 cm). Contact angle between the water droplet and the samples were automatically taken by the machine. The experiments were performed at 26 °C and about 60% relative humidity.

2.6. In vitro cell culture studies

2.6.1. Cytocompatibility and cell proliferation

The cytocompatibility and cell proliferation were investigated with HaCat keratinocytes (Passage-24), 3T3 Fibroblasts (ATCC CRL-1658, Passage-28), and EA.hy926 endothelial cells (ATCC CRL-2922, Passage-17). Cells were seeded on PHBV meshes and hybrid patches with 1 × 1 cm dimensions at a density of 2 × 10^4 cells/sample and cultured in 24-well plates. The patches were sterilized by 70% ethanol treatment and UV irradiation (15 min). All cells were maintained in DMEM (Gibco, Ireland) containing 10% fetal bovine serum and 1% penicillin/streptomycin solution (Gibco, US origin). Cell seeded patches were kept up to 7 days in an incubator with 5% CO_2 at 37 °C. To assess the cytocompatibility of the cells on the developed membranes, Live/Dead staining (Molecular Probes, Invitrogen, USA) was carried out according to the manufacturer's instructions ($n = 3$). Cells proliferated over the patches were imaged using an Olympus, FV300 fluorescent microscope. Percentage of viable cells on the patches were calculated from the microscopic images using Eq. (2).

$$\text{Viable cells}\ (\%) = \text{Live cells/Total cells} \times 100 \quad (2)$$

For MTT assay, cell seeded membranes (as described in the case of Live/Dead staining) were kept in 5% CO_2 incubator up to 7 days, and MTT assay was performed as per the instructions of manufacturer (Molecular Probes, Invitrogen, USA). Absorbance of the solution was recorded at 570 nm using a microplate reader (Infinite F200 PRO, Tecan, Switzerland).

Viability of cells on the patches were calculated using Eq. (3).

$$\text{Cell viability}\ (\%) = (\text{OD of sample/OD of control}) \times 100 \quad (3)$$

2.6.2. In vitro wound healing scratch assay

The *in vitro* wound healing scratch test was performed using 3T3 fibroblasts, HaCat keratinocytes and EA.hy926 endothelial cells to determine the effect of EGF loaded patches on keratinocyte cell migration. In each independent experiments using different cell lines, cells were grown in 24-well cell culture plates in DMEM medium and the test was performed using previously reported protocol [62]. Briefly, after removing the medium, scratches were made on the confluent layer of cells over the plates using 100 μL pipet tips. After gentle washing to remove the floating cells, samples were placed over the scratches, fresh media was added and incubated in a CO_2 incubator (37 °C, 5% CO_2 supply). Images of the plates were captured with an inverted microscope (Leica DMi1) immediately after the experiment and after 18 h. *In vitro* wound healing (%) was determined by quantifying the cell free scratched area using Eq. (4).

$$\textit{In vitro}\ \text{wound healing}\ (\%) = (Wd^0 - Wd^t)/Wd^0 \quad (4)$$

Whereas Wd^0 *and* Wd^t are the average distance between scratch boarders soon after wounding procedure and after time 't' of treatment.

We also performed DAPI-Phalloidin staining of cells after the completion of experiment to see the variation in cell morphology.

2.7. Determination of the angiogenic potential of the patches

The ability of developed patches to induce angiogenesis was studied by chorioallantoic membrane (CAM) assay as described in the earlier reports [63,64]. Briefly, fertilized chicken eggs were purchased from Arab Qatari for Poultry Production, Shamal Road, Farm Street, Qatar and incubated for 4 days in an egg incubator (1502-Digital Sportsman, GQF Manufacturing Company Inc.). A 1.5 cm diameter window was created on the top of the eggshell to provide access to the CAM. Sterile samples of PHBV-GelMA and PHBV-GelMA-EGF hybrid patches were deposited on the CAM. The eggs were placed in the incubator for 24 h in a static position. After 24 h, the CAMs were observed under stereomicroscope (Stemi 508) for angiogenesis and photographs were taken. The number of junctions and the diameter of blood vessel were quantified using ImageJ software.

2.8. Evaluation of direct application and diabetic wound healing potential in rats

Male Sprague Dawley rats with average weight of 220 g were selected for the diabetic wound healing study. The rat breed used in this study was sourced from Kerala Veterinary and Animal Sciences University, Mannuthy, India. Wound healing study was performed by strictly adhering to the guidelines of CPCSEA established by the Ministry of Environment, Forests and Climate Change, Animal Welfare Division of Government of India and with the prior approval of Institutional animal ethics committee (No.602/PO/Re/S/2002/CPCSEA) of Pushpagiri Institute of Medical Sciences and Research Centre, Tiruvalla, Kerala, India.

Induction of diabetes in rats was achieved by the intraperitoneal injection of streptozotocin (40 mg/kg body weight, Sigma Aldrich, USA). Glucose level in blood was monitored to understand the successful development of diabetes in rats as described in our earlier report [45]. Rats were anaesthetized by the intraperitoneal administration of

ketamine hydrochloride (50 mg/kg) and xylazine (5 mg/kg). After surface disinfection with alcohol, two 1.5 × 1.5 cm skin excision wounds (full thickness) were created at distance of 3 cm from each other on the dorsal region of the rats. The patches were developed on the wound by *in situ* crosslinking of GelMA (Fig. 8A). Photographs of some of the key steps during the *in situ* development of the patch are given in Supporting Information, Fig. S5. Prior to the application, PHBV meshes (1.5 × 1.5 cm) were sterilized as reported in a previous publication [65]. GelMA solutions containing photoinitiator were prepared as described in Section 2.2. To produce bi-layered patch, PHBV meshes were immersed in PBS for 1 h. Then, 150 μL GelMA solution was applied over the wounds, wet PHBV membranes were placed over the GelMA droplet and gently pressed for 30 s to facilitate the infiltration of the solution into the pores of the membrane and obtain hybrid PHBV-GelMA patches over the wound. To get EGF loaded patches, EGF was loaded in GelMA solution in such a way that 100 ng/cm^2 EGF was present in hybrid patches (PHBV-GelMA-EGF). The GelMA in the hybrid patches was stabilized by UV crosslinking for 3 min using a Elipar™ DeepCure-S LED Curing Light at 5 cm distance. Wounds were covered with polyurethane film and dry nonadherent gauze. The wounds were then covered with a gauze bandage roll and an adhesive elastic bandage. Each day the outer dressings were removed and the wounds were visually inspected for the evidence of infection if any. Photographic images of the wounds were captured at regular intervals up to 30 days to understand the physical appearance and rate of wound contraction. The wound contraction (%) was quantified using Eq. (5).

$$\text{Wound contraction (\%)} = [(WA^0 - WA^t)/WA^0] \times 100 \quad (5)$$

where 'WA^0' is the area of wound at 0th day (same day of wound generation) and 'WA^t' is the area of wound at 't' days of healing.

Skin was excised from the healed area after 30 days of study and used for histopathological analysis. The sections were stained with hematoxylin and eosin and for cellular infiltration, re-epithelialization and angiogenesis with a Leica light microscope.

2.9. Statistical analysis

All the experiments were performed for minimum 3 times and the results were reported as mean ± S.D. The statistical analysis was performed using the un-paired Student's *t*-test using Graph-Pad QuickCalcs (https://www.graphpad.com/quickcalcs/ttest1.cfm). *P* value less than 0.05 was considered as statistically significant.

3. Results

3.1. Morphology of the patches

The morphology of uncoated PHBV membranes and PHBV-GelMA membranes were examined by SEM analysis. Neat PHBV membranes showed the presence of randomly oriented fibers with average diameter of 0.9 ± 0.6 μm (Fig. 1A). PHBV-GelMA showed the coating of PHBV fibers with GelMA hydrogel (Fig. 1B). The presence of GelMA coating over PHBV fibers considerably modified the fiber diameter as evident from Fig. 1C and D. GelMA infiltrated PHBV meshes showed 3.5 ± 1.8 μm diameter. Loading of different concentrations of EGF in GelMA did not influence the overall morphology or fiber diameter of patches (Data not shown).

3.2. XRD and FTIR analysis

The XRD patterns of the neat PHBV, crosslinked GelMA, PHBV-GelMA and PHBV-GelMA-EGF samples are shown in Fig. 2A. The peaks at 13.5^0 and 16.9^0 correspond to α phase of PHBV polymer [66]. The XRD profile of the GelMA showed only broad peak at 2θ angle 32^0 attributed to polymer networks as reported in an earlier study [67]. The PHBV-GelMA hybrid patches showed the prominent peaks of PHBV and GelMA (marked by arrows in Fig. 2A). We did not observe a remarkable difference in the XRD patterns of PHBV-GelMA and PHBV-GelMA-EGF patches. This is plausible because nanogram quantities of EGF cannot be detected from the background diffraction of polymers.

FTIR analysis of the patches in attenuated total reflectance (ATR) mode was performed to examine the surface chemistry of PHBV, GelMA, PHBV-GelMA and GeLMA-PHBV-EGF fibers (Fig. 2B). The prominent band present around 1747 cm^{-1} indicated the stretching vibration of ester carbonyl groups (C=O) of PHBV [68]. The band observed at 1452 cm^{-1} indicated the asymmetric deformation of methylene groups. Band at 1380 cm^{-1} was due to the symmetrical wagging of CH_3 groups. Another major band at 1177 cm^{-1} could be assigned to the amorphous regions of PHBV. In addition, characteristic bands of symmetric –C–O–C– stretching vibration were present from 650 cm^{-1} to 1200 cm^{-1} whereas the antisymmetric –C–O–C–stretching bands were observed between 1050 and 1160 cm^{-1}. Characteristic amide bands of gelatin was observed in the FTIR spectra of GelMA such as N—H stretching vibration around 3310 cm^{-1} for the amide A, C—H stretching vibration around 3063 cm^{-1} for amide B, C═O stretching vibration around 1657 cm^{-1} for amide I, N—H deformation band around 1555 cm^{-1} for amide II and N—H deformation band around 1239 cm^{-1} for amide III [69]. The presence of some of the major FTIR bands of GelMA and PHBV in hybrid patches indicated the successful coating of GelMA on the surface of the PHBV fibers in hybrid patches. Small quantities of EGF were not detectable in the FTIR spectra of PHBV-GelMA-EGF loaded patches.

3.3. Uniaxial tensile strength

Fig. 3A-D shows the tensile stress–strain curves and calculated tensile properties of the patches. PHBV meshes showed a characteristic stress–strain behavior with a linearly elastic region at low strain region and deformation before breaking. Elongation at break of pure PHBV meshes, PHBV-GelMA and PHBV-GelMA-EGF patches were between 130% and 160% without a statistically significant inter-group difference. However, ultimate tensile strength and Young's modulus of PHBV-GelMA and PHBV-GelMA-EGF were higher than that of bare PHBV meshes. PHBV meshes possessed an ultimate tensile stress of 1.62 ± 0.3 MPa. PHBV-GelMA and PHBV-GelMA-EGF patches showed an ultimate tensile stress of 3.14 ± 0.43 MPa and 2.46 ± 0.3 MPa, respectively. Furthermore, Young's moduli of GelMA infiltrated patches were higher than that of bare PHBV membranes. PHBV membranes possessed a Young's modulus of 7.34 ± 1.78 MPa. PHBV-GelMA and PHBV-GelMA-EGF patches showed a Young's moduli of 16.28 ± 2.75 MPa and 14.84 ± 2.52 MPa, respectively. Comparable tensile properties observed for PHBV-GelMA and PHBV-GelMA-EGF patches indicate that the addition of a small amount of EGF could not modify the overall tensile behavior of the patches. However, infiltration of GelMA significantly improved the tensile strength and modulus of PHBV which could be attributed to the adhesion of adjacent fibers at their junctions with the help of GelMA which facilitated the uniform stress transfer between fibers.

3.4. Swelling and surface hydrophilicity

The ability of developed wound healing patches to absorb wound exudates without causing tissue maceration is very important particularly for highly-exudating diabetic wounds. Results of swelling study of pure PHBV, PHBV-GelMA and PHBV-GelMA-EGF membranes are given in Fig. 4A. Bare PHBV membranes have shown a swelling between 20.5 ± 4.7% and 56.6 ± 6.5% during the entire experimental period. Infiltration of GelMA largely increased the swelling of the patches. As expected, incorporation of EGF did not modify the swelling of PHBV-GelMA patches.

The surface hydrophobicity of the patches can be determined from water contact angle measurement. Results of water contact angle

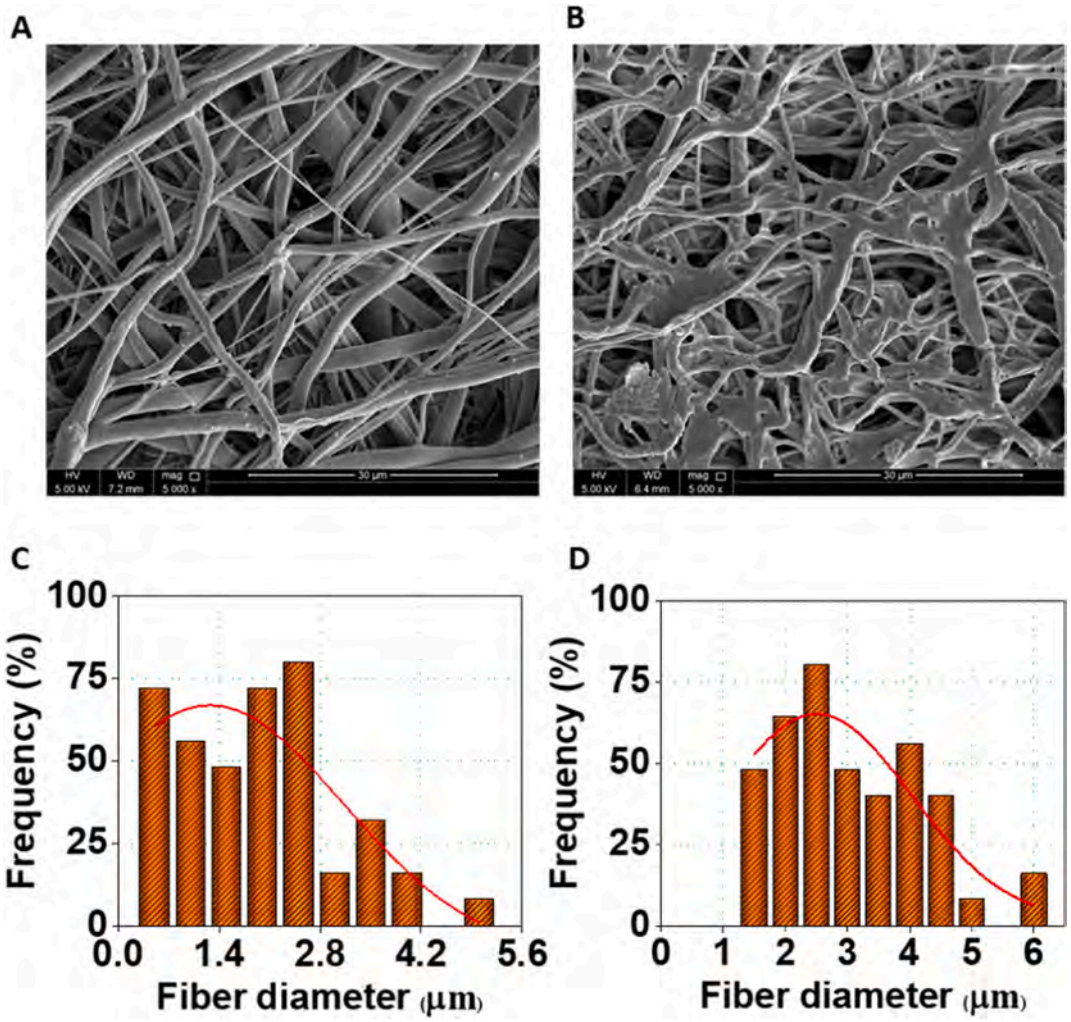

Fig. 1. Morphological characterization of developed PHBV mesh and PHBV-GelMA patch. SEM image showing the morphology of PHBV mesh (A) and PHBV-GelMA patch (B). Fiber diameter distribution graphs of PHBV mesh (C) and PHBV-GelMA patch (D).

measurements of pure PHBV meshes, PHBV-GelMA and PHBV-GelMA-EGF patches are given in Fig. 4B. Pure PHBV possessed a relatively high contact angle (106 ± 12°) as an indication of its high surface hydrophobicity. GelMA infiltration resulted in the decrease of contact angle to 47 ± 8° owing to a higher wettability of GelMA. PHBV-GelMA-EGF showed a comparable contact angle as in the case of PHBV-GelMA (44 ± 11°). This variation in hydrophilicity of the patches upon GelMA infiltration indirectly supports the successful modification of the PHBV meshes with GelMA.

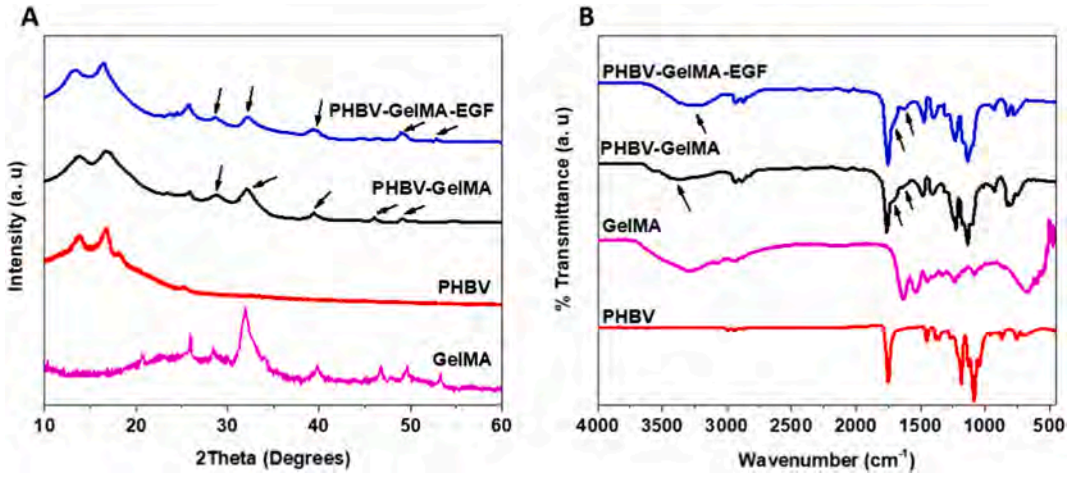

Fig. 2. Physical characterizations of PHBV mesh and hybrid patch. XRD patterns (A) and FTIR spectra (B) of fabricated hybrid patches and PHBV mesh and crosslinked GelMA.

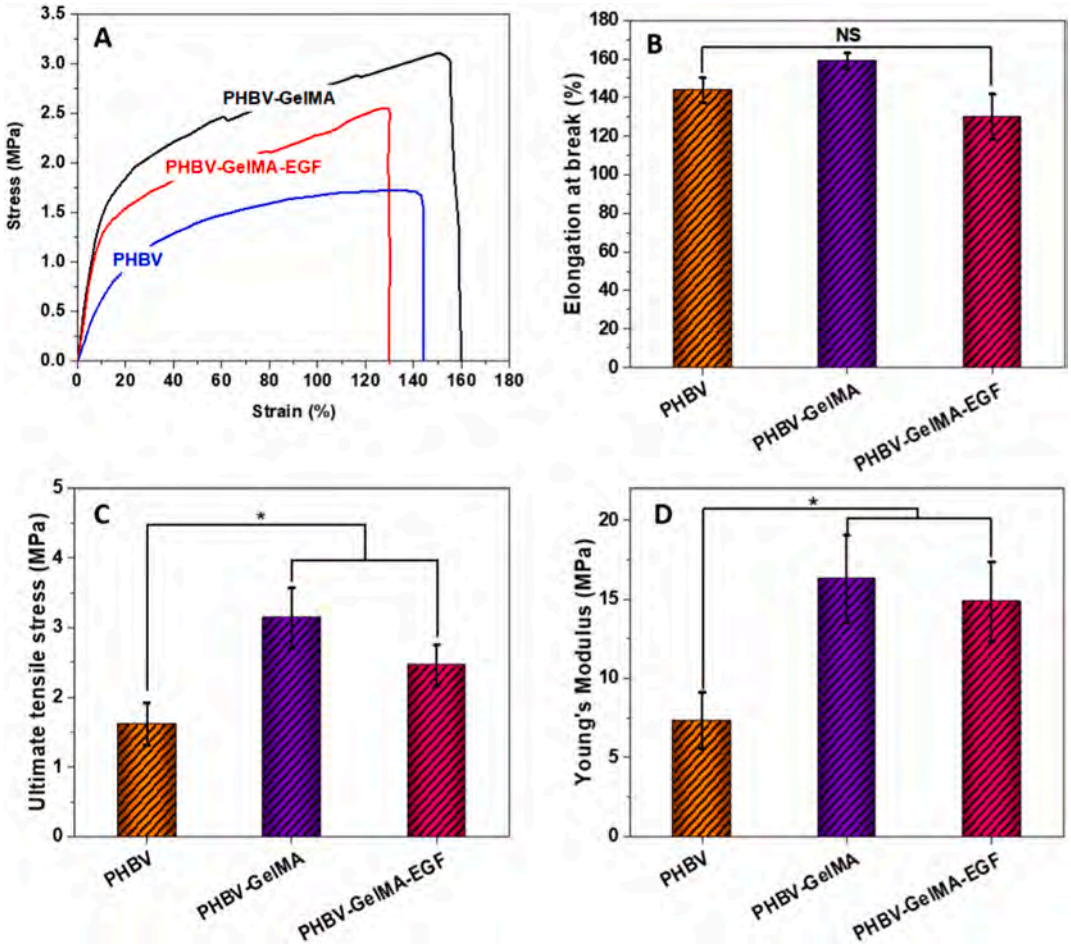

Fig. 3. Uniaxial tensile mechanical properties of the developed PHBV meshes and PHBV-GelMA hybrid patches. Stress-strain curve (A), Elongation at break (B), Ultimate tensile stress (C) and Young's modulus (D) of PHBV, PHBV-GelMA and PHBV-GelMA-EGF hybrid patches. P- values were obtained from Student's *t*-test where (*) indicates a statistically significant difference ($p \leq 0.05$) and NS indicates no statistically significant difference.

3.5. Cell viability and cell proliferation on the patches

To understand the cytocompatability of various types of mammalian cells on the developed patches, fibroblasts, keratinocytes and endothelial cells were grown on the patches and tested for cell viability and cell proliferation. Live/Dead test results are given in Fig. 5A (Quantification of viable cells from Live/Dead assay is given in Fig. S6). All tested cells were able to adhere and proliferate on bare PHBV meshes, but considerably less than those on the control tissue culture plates. Generally, adhesion and proliferation of all tested cells were higher on PHBV-GelMA patches compared to bare PHBV meshes. PHBV-GelMA-EGF patches showed relatively higher cell adhesion and

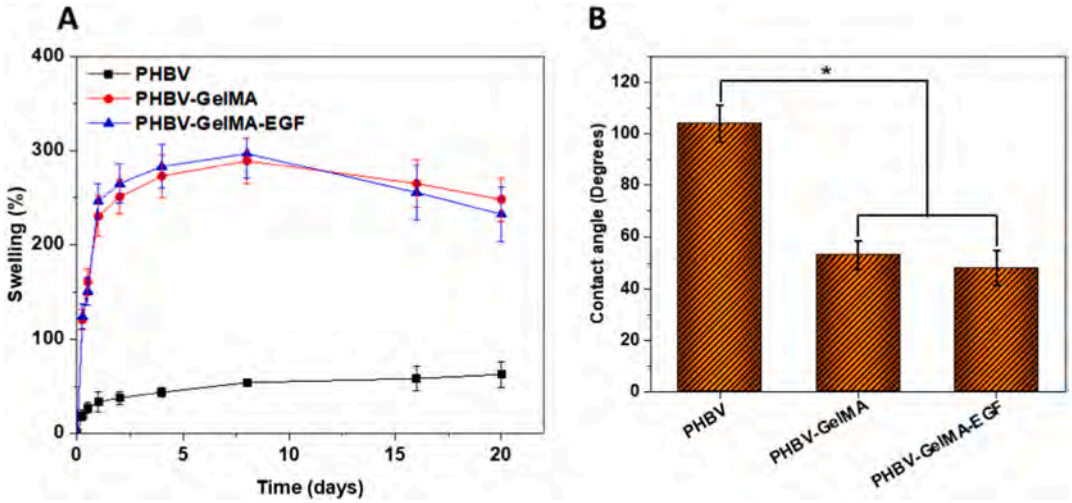

Fig. 4. Swelling of PHBV mesh, PHBV-GelMA and PHBV-GelMA-EGF hybrid patches (A). Water contact angle measurements on neat PHBV meshes, PHBV-GelMA and PHBV-GelMA-EGF hybrid patches (B). P- values were obtained from Student's t-test where (*) indicates a statistically significant difference ($p \leq 0.05$).

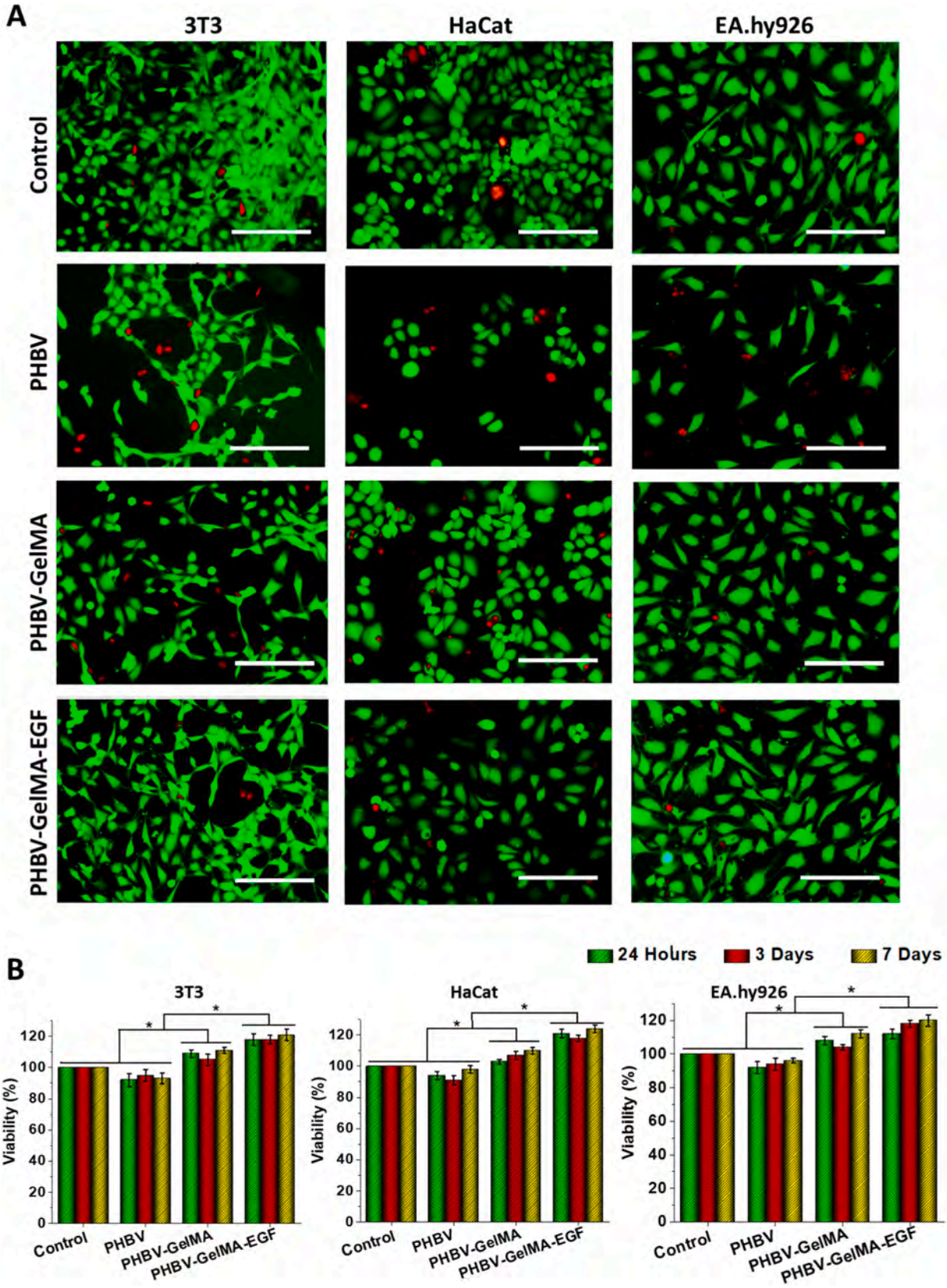

Fig. 5. Cytocompatibility and cell proliferation properties of developed patches. Live/Dead assay results indicating the adhesion and proliferation of fibroblast, keratinocyte and endothelial cells on PHBV, PHBV-GelMA and PHBV-GelMA-EGF patches (A). Results of MTT assay indicating the viability of 3T3 fibroblasts, HaCat keratinocytes and EA.hy926 endothelial cells which were grown in the presence of patches (B). (*) indicates the *P*-values where a statistically significant difference ($p \leq 0.05$) is present. Scale bars: 200 μm.

proliferation than PHBV-GelMA patches. Fibroblasts showed considerably higher cell proliferation on PHBV-GelMA-EGF compared to PHBV-GelMA patches. The difference in cell adhesion and proliferation between bare PHBV-GelMA-EGF and PHBV-GelMA hybrid patches was marginal in the case of keratinocyte cells. Endothelial cells showed higher cell adhesion and proliferation on PHBV-GelMA-EGF compared to PHBV-GelMA patches. However, the morphology of keratinocytes and endothelial cells cultured on PHBV-GelMA-EGF was considerably different compared to those cultured on PHBV-GelMA. Both cell lines became more elongated when cultured on EGF loaded patches. Conversely, in the case of fibroblast cells, despite the increased cell density, there was no visible difference in morphology when cultured on EGF loaded patches. Moreover, PHBV-GelMA and PHBV-GelMA-EGF showed the presence of only few dead cells (stained in red) in comparison with those observed on bare PHBV membranes. In addition, MTT cell viability assay was performed and the results are given in Fig. 5B to quantitatively measure cell proliferation in the presence of developed patches. Obtained results confirmed the improvement of cell proliferation when cultured in the presence of PHBV-GelMA and PHBV-GelMA-EGF patches.

3.6. In vitro cell migration and wound contraction potential of the patches

To investigate the ability of developed patches to promote cell migration and subsequent wound contraction, *in vitro* wound contraction test was performed [70] and the obtained results are given in Fig. 6 (A-C). Magnified views of the images are provided in Supporting Information, Figs. S7–S9. In the case of fibroblast cells, about 30% of wounded area were healed after 18 h of treatment in controls. Bare PHBV meshes also showed a similar trend of wound contraction. However, slightly higher wound contraction was detected for PHBV-GelMA patches ($P \leq 0.05$). Unlike other cell lines, statistically significant difference in wound contraction was observed for PHBV-GelMA treated HaCat cells. However, percentage of wound contraction for all tested cell lines were higher for PHBV-GelMA-EGF treatment groups (Fig. 6D). Cells that were treated with PHBV-GelMA-EGF patches showed elongated cell morphology, especially in the case of HaCat cells (Fig. 6E).

3.7. Proangiogenic effect of the patches

In order to understand the angiogenic potential of PHBV-GelMA-EGF patches, chicken embryo-based CAM assay was performed. Based on the obtained results of physicomechanical characterizations and *in vitro* cell culture experiments, we selected PHBV-GelMA and PHBV-GelMA-EGF patches for CAM angiogenesis test. Images of the CAM before and after the placement of the patches are provided in Fig. 7A. Quantitative measurement of fold increase of blood vessel junctions and

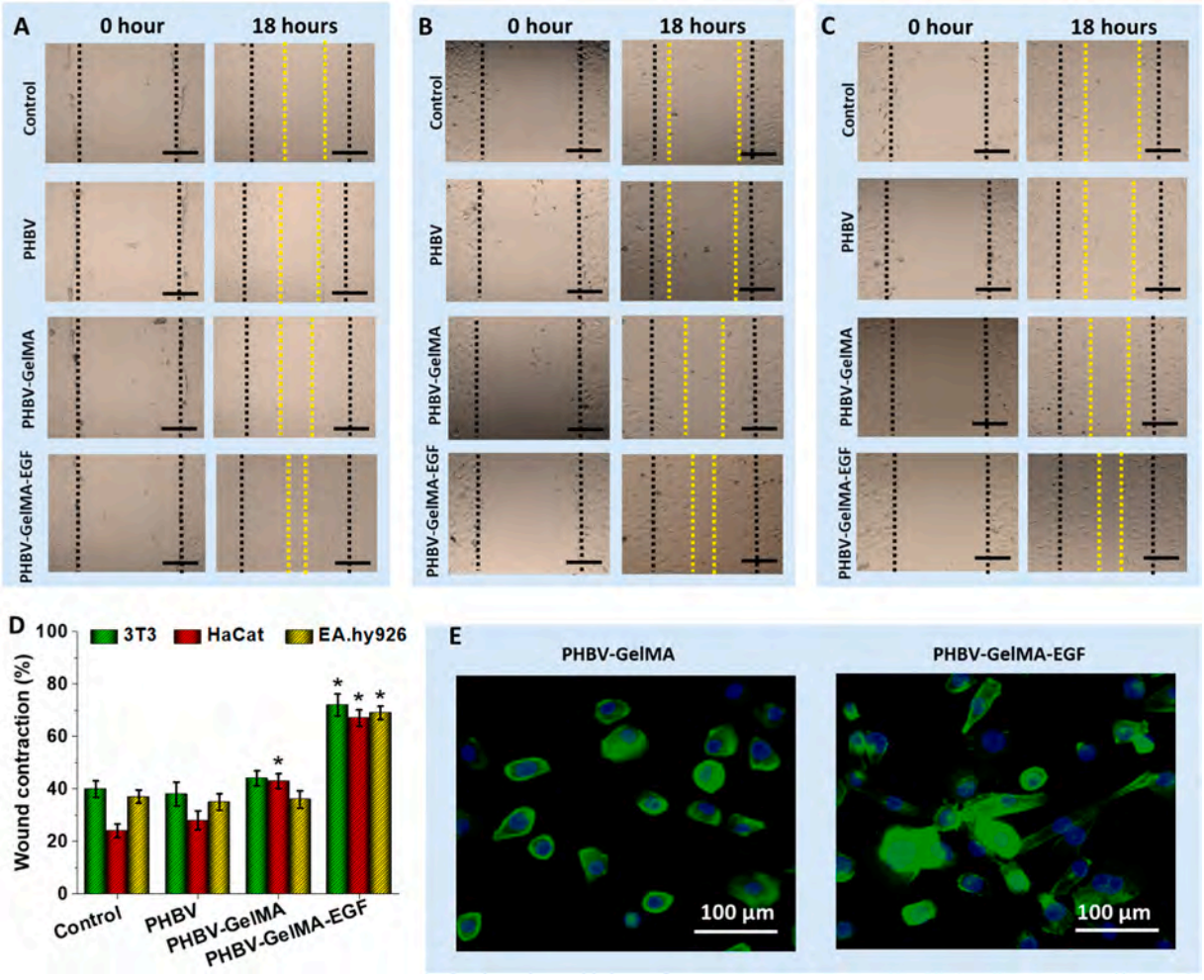

Fig. 6. Cell migration and wound contraction results of developed patches *in vitro* for 3T3 fibroblast (A), HaCat keratinocytes (B), and EA.hy926 endothelial cells (C). Percentage of wound contraction after incubation with the developed patches (D). Morphological differences in keratinocytes which were cultured with PHBV and hybrid patches with or without EGF (E). (*) indicates the P-values where a statistically significant difference ($p \leq 0.05$) is present. The images of *in vitro* wound healing were taken using 5× magnification (Scale bars: 500 µm). Black and Yellow dotted lines indicate the boundary of the wounds before sample treatment and after 18 h of treatment, respectively. (For interpretation of the references to colour in this figure legend, the reader is referred to the web version of this article.)

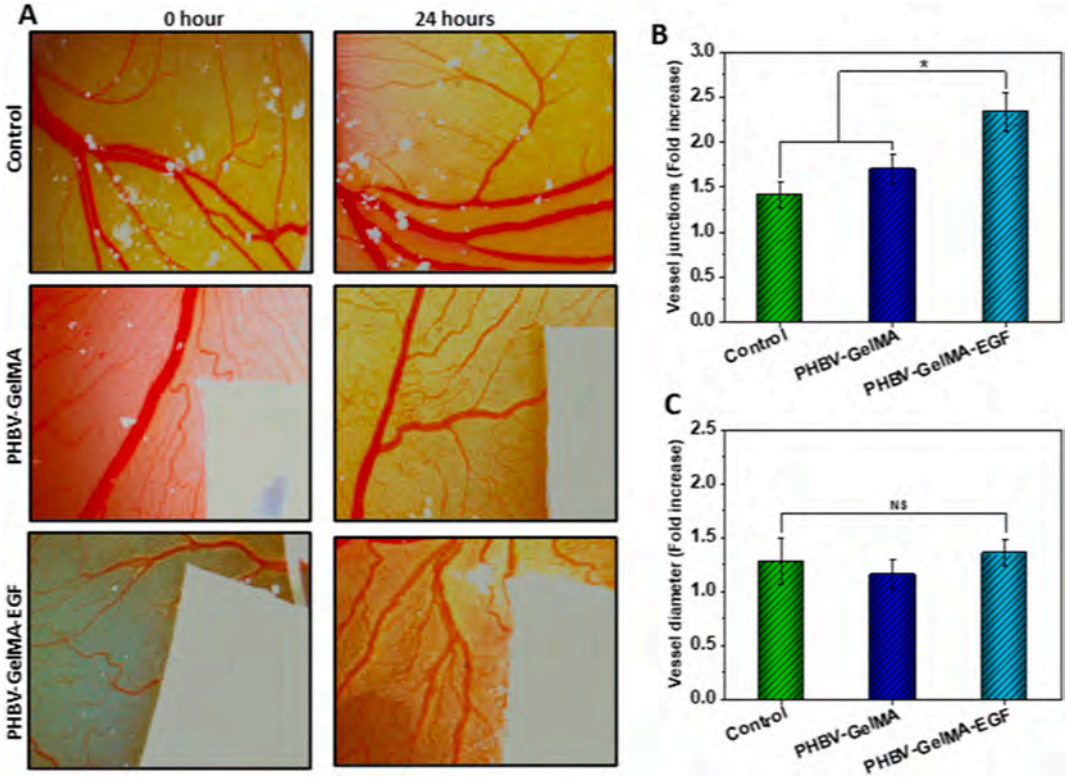

Fig. 7. Chicken chorioallantioic membrane angiogenesis assay. Photographs showing the angiogenic response after 24 h treatment with patches (A). Fold increase of junction (B) and fold increase of diameter (C) measured from the images of blood vessels. (*) indicates the P-values where a statistically significant difference ($p \leq 0.05$) is present. (NS) indicates no statistically significant difference.

blood vessel diameter is provided in Fig. 7B and C. Both controls and PHBV-GelMA patches showed relatively similar number of blood vessel junctions. PHBV-GelMA-EGF patches showed significantly higher number of capillary junctions compared to the controls and PHBV-GelMA treated groups ($P < 0.005$). There was no significant difference in blood vessel diameter between controls and different treatment groups.

3.8. Diabetic wound healing potential of hybrid patches

To investigate the *in situ* applicability and the effect of EGF loaded patches on diabetic wounds, the PHBV-GelMA and PHBV-GelMA-EGF patches were directly developed on the wounds by *in situ* crosslinking of GelMA on wounds in diabetic rats (Fig. 8A). Photographs of the wounds were taken soon after the application of the patch and every other day until the wound was completely healed. Wounds covered with PHBV-GelMA-EGF patches have shown higher rate of wound healing compared to PHBV-GelMA groups ($P \leq 0.05$) (Fig. 8B and C).

Histological examination of healed skin covered with hybrid patches showed the formation of an intact skin with epidermal and dermal structures (Fig. 8D). We did not observe very significant variation in the histological features of PHBV-GelMA and PHBV-GelMA-EGF patches. However, the healed wounds covered with PHBV-GelMA-EGF patches generated ra slightly thick epidermis.

4. Discussion

Many hydrogels and other biopolymers have been used to develop wound healing patches loaded with growth factors for the management of chronic wounds [71]. In this work, we developed a diabetic wound healing patch composed of GelMA as a soft layer loaded with EGF to support healing on electrospun PHBV meshes as mechanical barrier to protect the wound from the external environment. Developed patches showed excellent microbial barrier properties also (Supporting information, Table S1). The encapsulation of growth factors in protective hydrogel matrix from harsh wound microenvironments for chronic wound healing is well-studied in literature [72]. However, infiltration of photocrosslinkable GelMA hydrogel in electrospun membranes to develop constructs that release growth factors to facilitate cell proliferation, cell migration, angiogenesis and wound healing is a novel approach. Direct *in vivo* photocrosslinking of GelMA present in the hybrid patch upon application in the wound can ensure the integration of patch with the tissue without suturing.

PHBV-GelMA patches showed the effective coating of GelMA over PHBV fibers and the joining of fibers at their intersection. The GelMA coating largely increased the fiber diameter and changed the morphology of the fibers. It is plausible that a coating of hydrogel over the surface can increase the diameter of the fibers [73]. SEM analysis of the patches clearly showed the close integration of coating on the PHBV-fiber surface. It is worth mentioning that the produced hybrid patches could mimic the morphological features of the extracellular matrix since elastin [74] and collagen [75] fibers found in natural ECM share many structural features of the obtained fibers. This similarity may help to provide necessary physical cues for cell adhesion, proliferation, migration and result in rapid wound healing [76]. It is also interesting to note that the improved and adequate tensile strength, flexibility and elasticity of hybrid patches were comparable with that of skin and can provide mechanical fitness to the defective area and avoid failure during muscular movements. Higher tensile strength and modulus values that were observed for the hybrid patches can be ascribed on the binding interaction between the fibers and GelMA due to the gluing effect of GelMA at the contact points between fibers [77]. We also observed an improvement in swelling capacity and hydrophilicity of PHBV meshes upon infiltration of GelMA. Higher fluid uptake in the beginning of the experiment and subsequent limited uptake shown by bare PHBV meshes might be due to the retention of PBS inside the large

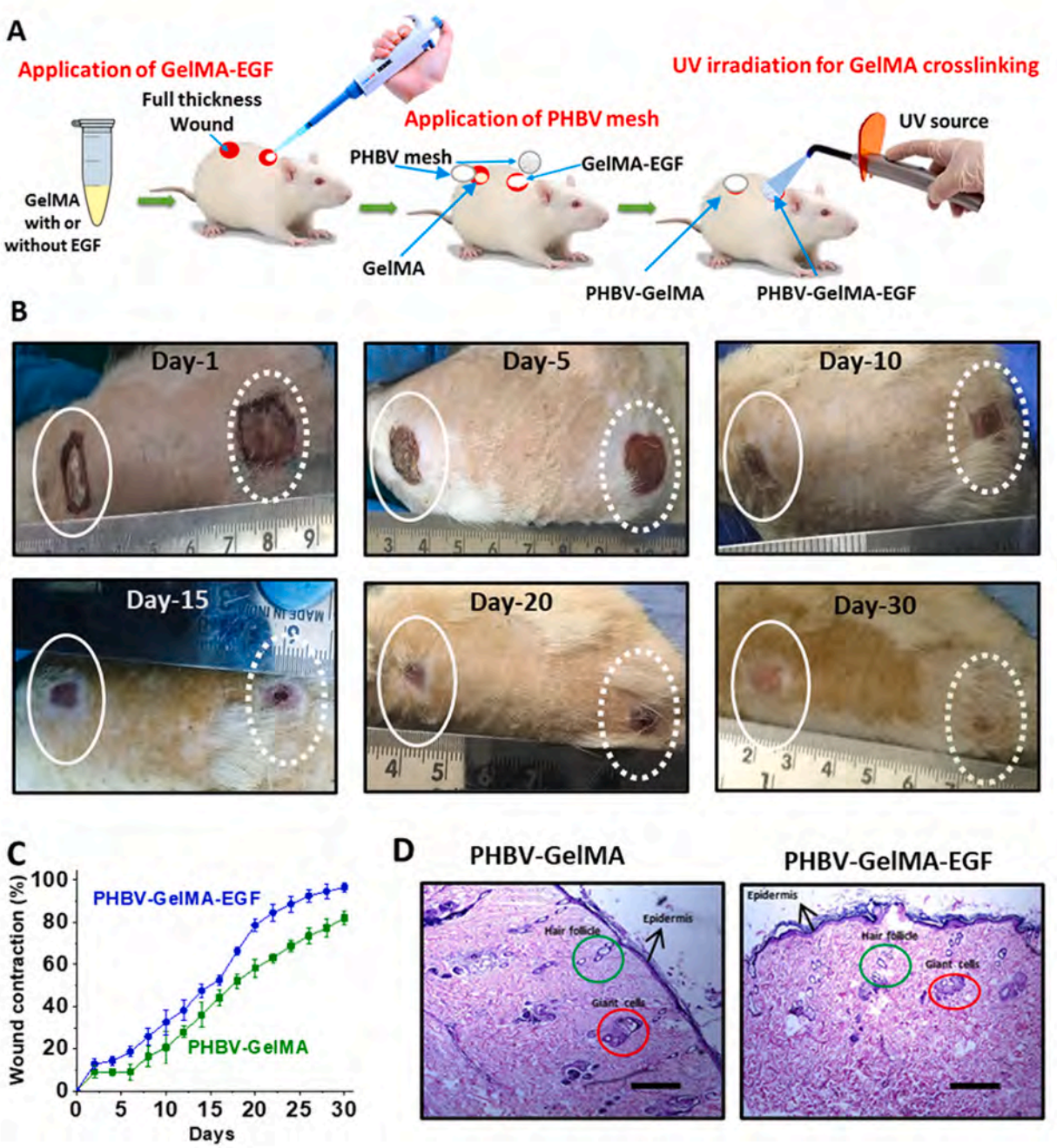

Fig. 8. Schematic representation showing the steps in wound healing evaluation of the patches (A). Representative photographs of the wounds covered with PHBV-GelMA and PHBV-GelMA-EGF hybrid patches showing the healing of full thickness excision wounds created on diabetic rats (B). Circles indicate PHBV-GelMA and doted circles indicate PHBV-GelMA-EGF hybrid patches. Rate of wound contraction (C) and the histological analysis of healed wound (D). Scale bars in histology images: 200 μm.

pore spaces of electrospun membranes. Higher fluid holding capacity of hybrid patches can be ascribed to the inherent hydrophilic nature of GelMA hydrogel present over PHBV fibers [78]. These findings are highly relevant towards wound healing applications of the hybrid patches because neither hydrophobic PHBV nor mechanically unstable GelMA can perform alone as a successful wound healing patch. In addition to the necessary exudate management capacity required in chronic wounds, higher cell proliferation and faster healing can be expected when such a hydrophilic patch is used on the wounds [73]. Earlier studies that indicate the positive impact of polymeric patches with hydrophilic property and exudate holding capacity on wound healing support our present findings [79].

It is essential to create an appropriate microenvironment with necessary cues for ensuring the proliferation of native cells migrating from wound edges towards the inner regions of the wound [16]. In order to promote cell proliferation and cell migration, we loaded EGF in GelMA hydrogel layer of the hybrid patches (PHBV-GelMA-EGF). Earlier studies also demonstrated that the GelMA hydrogel can perform as an excellent material to hold and slowly release biomolecules such as growth factors for wound healing applications [80]. The adhesion, proliferation and viability of native cells such as keratinocytes, fibroblasts and endothelial cells within the wound healing patch are crucial for ensuring the fast healing of chronic wounds [81,82]. As we hypothesized, the modification of PHBV membranes with GelMA hydrogel alone could improve the cell adhesion and proliferation up to a certain extent. However, incorporation of EGF resulted in the improvement of

cell proliferation and viability to a great extent. In corroboration with our results, other studies also indicated that EGF can protect cells from apoptosis and promote their proliferation [83–85]. We also observed a clear variation in cell morphology upon treatment with EGF loaded patches compared to other patches which could be due to the activation of several cell motility associated genes and resulting epithelial-mesenchymal transition (EMT) [86]. Cells that undergo EMT show an elongated mesenchymal like morphology [87]. As obvious, there was no distinguishable difference in cell morphology of fibroblasts treated with EGF loaded patches and controls as fibroblasts are already in mesenchymal phenotype [88]. EMT has a pronounced role in cell migration and wound healing [89]. EGF loaded patches produced a pronounced effect on the migration of all tested cells and resulted in fast contraction of the experimentally created *in vitro* wounds. EGF has already been reported for its ability to produce a positive impact on the growth and migration of several types of mammalian cells such as oral epithelial cells [90], enterocytes [91], keratinocytes [92,93] and endothelial cells [94,95]. Upon treatment with EGF loaded hybrid patches, cells (especially keratinocytes) showed a very pronounced variation in cell morphology (elongated morphology) during cell migration indicating EMT [96]. Since extent of re-epithelialization of wounds including chronic diabetic wounds depends upon the rate of cell migration from the margins of the wound, developed patches loaded with EGF with excellent cell migratory potential can be a good candidate for diabetic wound healing applications.

Insufficient angiogenesis worsens the chronicity of diabetic wounds [97]. Higher angiogenesis was observed on CAM treated with EGF loaded patches. Other studies also indicated that EGF can promote angiogenesis [98,99]. Higher endothelial cell migration, proliferation and survival are required for mitigating impaired angiogenesis in diabetic wounds [100]. Higher viability and migration of endothelial cells might have played a major role in the observed higher angiogenesis response in chicken embryo CAM model. As evident from other studies, EGF might also have induced VEGF, a master regulator in angiogenesis, expression inother native cells in chicken embryo that resulted in increased angiogenesis [101].

Our experiments revealed that PHBV-GelMA-EGF can produce faster wound closure than those patches without EGF. Observed higher diabetic wound healing might be due to the increased cell migration and cell proliferation induced by EGF as evident from our *in vitro* studies and other reported works [101,102]. It is interesting to note that the obtained results were comparable to that of diabetic wound healing rate observed when umbilical cord perivascular cell seeded acellulardermal matrix was used [103]. Obtained results for PHBV-GelMA-EGF were also comparable or slightly superior to that of exosome loaded hydrogel patches [104]. The histology showed a marginally higher epithelization in the PHBV-GelMA-EGF treated healed wounds compared to the PHBV-GelMA treated healed wounds. Moreover, in both cases, healed skin tissues showed almost complete re-epithelialization and formation of dermal tissues. Our earlier study clearly showed that a very thin epidermis and unorganized hypodermis were only formed when PHBV membranes alone were applied on the wounds [45]. However, compared to the normal rat skin, a slightly thin epidermis was only formed in the healed skin tissue which were covered with hybrid patches [45]. This was expected due tothe fact that complete remodeling of skin can take several months. Moreover, it is almost impossible to achieve the complete regeneration of the original form and function of original skin by currently available approaches. However, fibrotic scars, which impairs normal tissue organization and aesthetics, were minimum after the complete healing of wounds which were treated with the hybrid patches.

Based on the obtained results of detailed physicomechanical and biological characterization, we propose that EGF loaded PHBV-GelMA hybrid patches with their flexible morphological features, good mechanical properties, ability to provide a niche for cell adhesion/proliferation and cues for vascularization, are an effective candidate for diabetic wound healing applications. It was noteworthy that a small quantity of EGF in the PHBV-GelMA-EGF patches could provide a considerable improvement in the overall performance, suggesting their applicability as a cost-effective patch to effectively manage diabetic wounds. Although this work provides a detailed investigation with experimental evidence to show the application potential of PHBV-GelMA-EGF based patch for diabetic wound healing, a deeper investigation is still needed to understand the potential systemic effect of photoinitiator and other components directly exposed to the wound during the application.

5. Conclusions

In this work, hybrid wound healing patches based on electrospun PHBV meshes, GelMA and EGF were developed and thoroughly characterized for physicochemical properties, *in vitro* biological performance and *in vivo* wound healing potential. SEM analysis indicated that the developed patches were highly porous with the coating of GelMA. XRD and FTIR analyses demonstrated the formation of hybrid structured patches. Compared to bare PHBV meshes, hybrid patches showed optimal elasticity, tensile strength, and tensile modulus as suitable for wound healing applications. GelMA infiltrated hybrid patches showed higher exudate uptake capacity and hydrophilicity which are important for chronic wound healing applications. Higher fibroblasts, keratinocytes and endothelial cell proliferation and viability was observed upon treatment with EGF loaded hybrid patches. Hybrid patches loaded with EGF facilitated higher cell migration and resulted in fast *in vitro* wound closure. Compared to bare PHBV membranes, PHBV-GelMA patches and controls, EGF incorporated hybrid patches produced improved angiogenesis. Overall results indicate that EGF loaded GelMA hydrogels supported by PHBV meshes can be used as excellent diabetic wound healing patches. Finally, results of wound healing experiments using diabetic rats clearly showed the ability of EGF containing hybrid patches to enhance diabetic wound healing. Corroborating the desirable morphological features, mechanical properties, exudate management capacity, higher cell proliferation, proangiogenic property and ability to promote rapid diabetic wound healing, the developed PHBV-GelMA-EGF hybrid patches are highly promising for diabetic wound healing applications.

CRediT authorship contribution statement

Conceptualization: R.A (Robin Augustine)., A.H. Investigation: R.A (Robin Augustine)., Sample characterization: R.A (Robin Augustine)., S.R.U.R., Animal studies: Y.B.D., R.V., R.A (Robin Augustine). Histology: R.N.U. Resources: A.H., S.T. Writing—original draft preparation: R.A (Robin Augustine). Writing—review and editing: R.A (Robin Augustine)., A.H., H.C.Y., R.A (Rashad Alfkey), S.T., A.E.M. Visualization: R.A (Robin Augustine). Supervision: A.H., A.E.M. Project coordination: R.A. Funding acquisition: A.H. All authors have read and agreed to the published version of the manuscript.

Declaration of competing interest

Authors declare that there's no financial/personal interest or belief that could affect the results, discussions or conclusions which are reported in this work.

Acknowledgments

This article was made possible by the NPRP9-144-3-021 grant funded by Qatar National Research Fund (a part of Qatar Foundation). The statements made here are the sole responsibility of the authors. We also acknowledge the support provided by the Central Laboratories Unit (CLU), Qatar University, Doha, Qatar. The publication of this article

was funded by the Qatar National Library.

Appendix A. Supplementary data

Supplementary data to this article can be found online at https://doi.org/10.1016/j.msec.2020.111519.

References

[1] R.G. Frykberg, T. Zgonis, D.G. Armstrong, V.R. Driver, J.M. Giurini, S.R. Kravitz, A.S. Landsman, L.A. Lavery, J.C. Moore, J.M. Schuberth, D.K. Wukich, C. Andersen, J.V. Vanore, Diabetic foot disorders: a clinical practice guideline (2006 revision), J. Foot Ankle Surg. 45 (2006) S1–66, https://doi.org/10.1016/S1067-2516(07)60001-5.

[2] M. Mutluoglu, G. Uzun, M. Bennett, P. Germonpré, D. Smart, D. Mathieu, Poorly designed research does not help clarify the role of hyperbaric, Diving Hyperb. Med. 46 (2016) 2–4 http://www.ncbi.nlm.nih.gov/pubmed/27723012.

[3] L. Mosonyi, Diabetes Mellitus and Insipidus, Br. Med. J. 2 (1964) 1009, https://doi.org/10.1136/bmj.2.5415.1009-a.

[4] A.I. Vinik, Diabetic sensory and motor neuropathy, N. Engl. J. Med. 374 (2016) 1455–1464, https://doi.org/10.1056/nejmcp1503948.

[5] J. Tongers, J.G. Roncalli, D.W. Losordo, Therapeutic angiogenesis for critical limb ischemia: microvascular therapies coming of age, Circulation. 118 (2008) 9–16, https://doi.org/10.1161/CIRCULATIONAHA.108.784371.

[6] A.L. Laiva, F.J. O'Brien, M.B. Keogh, Innovations in gene and growth factor delivery systems for diabetic wound healing, J. Tissue Eng. Regen. Med. 12 (2018) e296–e312, https://doi.org/10.1002/term.2443.

[7] S. Barrientos, O. Stojadinovic, M.S. Golinko, H. Brem, M. Tomic-Canic, Growth factors and cytokines in wound healing, Wound Repair Regen. 16 (2008) 585–601, https://doi.org/10.1111/j.1524-475X.2008.00410.x.

[8] R. Augustine, A.A. Zahid, A. Hasan, M. Wang, T.J. Webster, Ctgf loaded electrospun dual porous core-shell membrane for diabetic wound healing, Int. J. Nanomedicine 14 (2019) 8573–8588, https://doi.org/10.2147/IJN.S224047.

[9] A. Haumer, P.E. Bourgine, P. Occhetta, G. Born, R. Tasso, I. Martin, Delivery of cellular factors to regulate bone healing, Adv. Drug Deliv. Rev. 129 (2018) 285–294, https://doi.org/10.1016/j.addr.2018.01.010.

[10] J. Berlanga-Acosta, Diabetic lower extremity wounds: the rationale for growth factors-based infiltration treatment, Int. Wound J. 8 (2011) 612–620, https://doi.org/10.1111/j.1742-481X.2011.00840.x.

[11] R.J. Bodnar, Epidermal growth factor and epidermal growth factor receptor: the Yin and Yang in the treatment of cutaneous wounds and cancer, Adv. Wound Care. 2 (2013) 24–29, https://doi.org/10.1089/wound.2011.0326.

[12] J. Berlanga-Acosta, J. Fernández-Montequín, C. Valdés-Pérez, W. Savigne-Gutiérrez, Y. Mendoza-Marí, A. García-Ojalvo, V. Falcón-Cama, D. García del Barco-Herrera, M. Fernández-Mayola, H. Pérez-Saad, E. Pimentel-Vázquez, A. Urquiza-Rodríguez, M. Kulikovsky, G. Guillén-Nieto, Diabetic foot ulcers and epidermal growth factor: revisiting the local delivery route for a successful outcome, Biomed. Res. Int. 2017 (2017) 1–10, https://doi.org/10.1155/2017/2923759.

[13] N. Masood, R. Ahmed, M. Tariq, Z. Ahmed, M.S. Masoud, I. Ali, R. Asghar, A. Andleeb, A. Hasan, Silver nanoparticle impregnated chitosan-PEG hydrogel enhances wound healing in diabetes induced rabbits, Int. J. Pharm. 559 (2019) 23–36, https://doi.org/10.1016/j.ijpharm.2019.01.019.

[14] R. Ahmed, M. Tariq, I. Ali, R. Asghar, P. Noorunnisa Khanam, R. Augustine, A. Hasan, Novel electrospun chitosan/polyvinyl alcohol/zinc oxide nanofibrous mats with antibacterial and antioxidant properties for diabetic wound healing, Int. J. Biol. Macromol. 120 (2018) 385–393, https://doi.org/10.1016/j.ijbiomac.2018.08.057.

[15] R. Augustine, R. Rajendran, U. Cvelbar, M. Mozetič, A. George, Biopolymers for Health, Food, and Cosmetic Applications, in: Handb. Biopolym. Mater. From Blends Compos. to Gels Complex Networks, 2013: pp. 801–849. doi:https://doi.org/10.1002/9783527652457.ch27.

[16] R. Augustine, N. Kalarikkal, S. Thomas, Advancement of wound care from grafts to bioengineered smart skin substitutes, Prog. Biomater. 3 (2014) 103–113, https://doi.org/10.1007/s40204-014-0030-y.

[17] A.A. Zahid, R. Ahmed, S. Raza ur Rehman, R. Augustine, M. Tariq, A. Hasan, Nitric oxide releasing chitosan-poly (vinyl alcohol) hydrogel promotes angiogenesis in chick embryo model, Int. J. Biol. Macromol. 136 (2019) 901–910. doi:https://doi.org/10.1016/j.ijbiomac.2019.06.136.

[18] B.D. Kevadiya, G.V. Joshi, H.M. Mody, H.C. Bajaj, Biopolymer-clay hydrogel composites as drug carrier: host-guest intercalation and in vitro release study of lidocaine hydrochloride, Appl. Clay Sci. 52 (2011) 364–367, https://doi.org/10.1016/j.clay.2011.03.017.

[19] B.D. Kevadiya, S. Rajkumar, H.C. Bajaj, S.S. Chettiar, K. Gosai, H. Brahmbhatt, A.S. Bhatt, Y.K. Barvaliya, G.S. Dave, R.K. Kothari, Biodegradable gelatin-ciprofloxacin-montmorillonite composite hydrogels for controlled drug release and wound dressing application, Colloids Surfaces B Biointerfaces. 122 (2014) 175–183, https://doi.org/10.1016/j.colsurfb.2014.06.051.

[20] A.A. Zahid, R. Ahmed, S.R.U. Rehman, R. Augustine, A. Hasan, Enhanced Angiogenesis with Nitric Oxide Releasing Chitosan-PVA Hydrogel for Wound Healing, in: Trans, Annu. Meet. Soc. Biomater. Annu. Int. Biomater. Symp. (2019).

[21] Y. Wang, L. Shang, G. Chen, L. Sun, X. Zhang, Y. Zhao, Bioinspired structural color patch with anisotropic surface adhesion, Sci. Adv. 6 (2020). doi:https://doi.org/10.1126/sciadv.aax8258.

[22] H. Wang, Y. Liu, Z. Chen, L. Sun, Y. Zhao, Anisotropic structural color particles from colloidal phase separation, Sci. Adv. 6 (2020). doi:https://doi.org/10.1126/sciadv.aay1438.

[23] H. Huang, Y. Yu, Y. Hu, X. He, O. Berk Usta, M.L. Yarmush, Generation and manipulation of hydrogel microcapsules by droplet-based microfluidics for mammalian cell culture, Lab Chip 17 (2017) 1913–1932, https://doi.org/10.1039/c7lc00262a.

[24] E.A. Kamoun, E.R.S. Kenawy, X. Chen, A review on polymeric hydrogel membranes for wound dressing applications: PVA-based hydrogel dressings, J. Adv. Res. 8 (2017) 217–233, https://doi.org/10.1016/j.jare.2017.01.005.

[25] S.R.U. Rehman, R. Augustine, A.A. Zahid, R. Ahmed, A. Hasan, Reduced Graphene Oxide Impregnated Gelma Hydrogel Promotes Angiogenic Activity in Chick Embryo Model, in: Trans, Annu. Meet. Soc. Biomater. Annu. Int. Biomater. Symp. (2019).

[26] B.J. Klotz, D. Gawlitta, A.J.W.P. Rosenberg, J. Malda, F.P.W. Melchels, Gelatin-methacryloyl hydrogels: towards biofabrication-based tissue repair, Trends Biotechnol. 34 (2016) 394–407, https://doi.org/10.1016/j.tibtech.2016.01.002.

[27] D. Loessner, C. Meinert, E. Kaemmerer, L.C. Martine, K. Yue, P.A. Levett, T.J. Klein, F.P.W. Melchels, A. Khademhosseini, D.W. Hutmacher, Functionalization, preparation and use of cell-laden gelatin methacryloyl-based hydrogels as modular tissue culture platforms, Nat. Protoc. 11 (2016) 727, https://doi.org/10.1038/nprot.2016.037.

[28] K.S. Lim, B.J. Klotz, G.C.J. Lindberg, F.P.W. Melchels, G.J. Hooper, J. Malda, D. Gawlitta, T.B.F. Woodfield, Visible Light Cross-Linking of Gelatin Hydrogels Offers an Enhanced Cell Microenvironment with Improved Light Penetration Depth, Macromol. Biosci. 19 (2019). doi:https://doi.org/10.1002/mabi.201900098.

[29] S. Mohammadi, S. Ramakrishna, S. Laurent, M.A. Shokrgozar, D. Semnani, D. Sadeghi, S. Bonakdar, M. Akbari, Fabrication of nanofibrous PVA/alginate-sulfate substrates for growth factor delivery, J. Biomed. Mater. Res. Part A. 107 (2019) 403–413, https://doi.org/10.1002/jbm.a.36552.

[30] K. Rahimi Mamaghani, S. Morteza Naghib, A. Zahedi, M. Mozafari, Synthesis and microstructural characterization of GelMa/PEGDA hybrid hydrogel containing graphene oxide for biomedical purposes, Mater. Today Proc. 5 (2018) 15635–15644, https://doi.org/10.1016/j.matpr.2018.04.173.

[31] F. Fu, L. Shang, F. Zheng, Z. Chen, H. Wang, J. Wang, Z. Gu, Y. Zhao, Cells cultured on Core-Shell photonic crystal barcodes for drug screening, ACS Appl. Mater. Interfaces 8 (2016) 13840–13848, https://doi.org/10.1021/acsami.6b04966.

[32] J.W. Nichol, S.T. Koshy, H. Bae, C.M. Hwang, S. Yamanlar, A. Khademhosseini, Cell-laden microengineered gelatin methacrylate hydrogels, Biomaterials. 31 (2010) 5536–5544, https://doi.org/10.1016/j.biomaterials.2010.03.064.

[33] V.H.M. Mouser, F.P.W. Melchels, J. Visser, W.J.A. Dhert, D. Gawlitta, J. Malda, Yield stress determines bioprintability of hydrogels based on gelatin-methacryloyl and gellan gum for cartilage bioprinting, Biofabrication. 8 (2016). doi:https://doi.org/10.1088/1758-5090/8/3/035003.

[34] K.R. Mamaghani, S.M. Naghib, A. Zahedi, M. Rahmanian, M. Mozafari, GelMa/PEGDA containing graphene oxide as an IPN hydrogel with superior mechanical performance, in: Mater. Today Proc., 2018: pp. 15790–15799. doi:https://doi.org/10.1016/j.matpr.2018.04.193.

[35] I.K. Ko, S.J. Lee, A. Atala, J.J. Yoo, In situ tissue regeneration through host stem cell recruitment, Exp. Mol. Med. 45 (2013) e57, , https://doi.org/10.1038/emm.2013.118.

[36] A. Paul, A. Hasan, H. Al Kindi, A.K. Gaharwar, V.T.S. Rao, M. Nikkhah, S.R. Shin, D. Krafft, M.R. Dokmeci, D. Shum-Tim, A. Khademhosseini, Injectable graphene oxide/hydrogel-based angiogenic gene delivery system for vasculogenesis and cardiac repair, ACS Nano 8 (2014) 8050–8062, https://doi.org/10.1021/nn5020787.

[37] A. Hasan, S. Soliman, F. El Hajj, Y.T. Tseng, H.C. Yalcin, H.E. Marei, Fabrication and in vitro characterization of a tissue engineered PCL-PLLA heart valve, Sci. Rep. 8 (2018) 8187, https://doi.org/10.1038/s41598-018-26452-y.

[38] D. da Silva, M. Kaduri, M. Poley, O. Adir, N. Krinsky, J. Shainsky-Roitman, A. Schroeder, Biocompatibility, biodegradation and excretion of polylactic acid (PLA) in medical implants and theranostic systems, Chem. Eng. J. 340 (2018) 9–14, https://doi.org/10.1016/J.CEJ.2018.01.010.

[39] H.S. Kim, J. Chen, L.P. Wu, J. Wu, H. Xiang, K.W. Leong, J. Han, Prevention of excessive scar formation using nanofibrous meshes made of biodegradable elastomer poly(3-hydroxybutyrate-co-3-hydroxyvalerate), J. Tissue Eng. 11 (2020). doi:https://doi.org/10.1177/2041731420949332.

[40] H. Liu, M. Pancholi, J. Stubbs, D. Raghavan, Influence of hydroxyvalerate composition of polyhydroxy butyrate valerate (PHBV) copolymer on bone cell viability and in vitro degradation, J. Appl. Polym. Sci. 116 (2010) 3225–3231, https://doi.org/10.1002/app.31915.

[41] M. Kouhi, M. Fathi, M.P. Prabhakaran, M. Shamanian, S. Ramakrishna, Enhanced proliferation and mineralization of human fetal osteoblast cells on PHBV-bredigite nanofibrous scaffolds, Mater. Today Proc. 5 (2018) 15702–15709, https://doi.org/10.1016/J.MATPR.2018.04.181.

[42] B. Veleirinho, D.S. Coelho, P.F. Dias, M. Maraschin, R.M. Ribeiro-do-Valle, J.A. Lopes-da-Silva, Nanofibrous poly(3-hydroxybutyrate-co-3-hydroxyvalerate)/chitosan scaffolds for skin regeneration, Int. J. Biol. Macromol. 51 (2012) 343–350, https://doi.org/10.1016/j.ijbiomac.2012.05.023.

[43] P. Kuppan, K.S. Vasanthan, D. Sundaramurthi, U.M. Krishnan, S. Sethuraman, Development of poly(3-hydroxybutyrate-co-3-hydroxyvalerate) fibers for skin tissue engineering: effects of topography, mechanical, and chemical stimuli, Biomacromolecules. 12 (2011) 3156–3165, https://doi.org/10.1021/bm200618w.

[44] L.Y. Wang, Y.J. Wang, D.R. Cao, Surface modification of poly(3-hydroxybutyrate-

co-3-hydroxyvalerate) membrane by combining surface aminolysis treatment with collagen immobilization, J. Macromol. Sci. Part A Pure Appl. Chem. 46 (2009) 765–773, https://doi.org/10.1080/10601320903004517.
[45] R. Augustine, A. Hasan, N.K. Patan, Y.B. Dalvi, R. Varghese, A. Antony, R.N. Unni, N. Sandhyarani, A.E. Al Moustafa, Cerium oxide nanoparticle incorporated electrospun poly(3-hydroxybutyrate-co-3-hydroxyvalerate) membranes for diabetic wound healing applications, ACS Biomater. Sci. Eng. 6 (2020) 58–70, https://doi.org/10.1021/acsbiomaterials.8b01352.
[46] P.P. Mahamuni-Badiger, P.M. Patil, P.R. Patel, M.J. Dhanavade, M.V. Badiger, Y.N. Marathe, R.A. Bohara, R.A. Bohara, Electrospun poly(3-hydroxybutyrate-: co -3-hydroxyvalerate)/polyethylene oxide (PEO) microfibers reinforced with ZnO nanocrystals for antibacterial and antibiofilm wound dressing applications, New J. Chem. 44 (2020) 9754–9766, https://doi.org/10.1039/d0nj01384f.
[47] K. Ghosal, C. Agatemor, Z. Špitálsky, S. Thomas, E. Kny, Electrospinning tissue engineering and wound dressing scaffolds from polymer-titanium dioxide nanocomposites, Chem. Eng. J. 358 (2019) 1262–1278, https://doi.org/10.1016/j.cej.2018.10.117.
[48] R. Augustine, A. Hasan, N.K. Patan, A. Augustine, Y.B. Dalvi, R. Varghese, R.N. Unni, N. Kalarikkal, A.E. Al Moustafa, S. Thomas, Titanium nanorods loaded PCL meshes with enhanced blood vessel formation and cell migration for wound dressing applications, Macromol. Biosci. 24 (2019) 101–123, https://doi.org/10.1002/mabi.201900058.
[49] R. Augustine, E.A. Dominic, I. Reju, B. Kaimal, N. Kalarikkal, S. Thomas, Electrospun polycaprolactone membranes incorporated with ZnO nanoparticles as skin substitutes with enhanced fibroblast proliferation and wound healing, RSC Adv. 4 (2014). doi:https://doi.org/10.1039/c4ra02450h.
[50] B. Joseph, R. Augustine, N. Kalarikkal, S. Thomas, B. Seantier, Y. Grohens, Recent advances in electrospun polycaprolactone based scaffolds for wound healing and skin bioengineering applications, Mater. Today Commun. 19 (2019) 319–335, https://doi.org/10.1016/j.mtcomm.2019.02.009.
[51] M. Ranjbar Mohammadi, S. Kargozar, S.H. Bahrami, S. Rabbani, An excellent nanofibrous matrix based on gum tragacanth-poly (Ɛ-caprolactone)-poly (vinyl alcohol) for application in diabetic wound healing, Polym. Degrad. Stab. 174 (2020). doi:https://doi.org/10.1016/j.polymdegradstab.2020.109105.
[52] A. Augustine, R. Augustine, A. Hasan, V. Raghuveeran, D. Rouxel, N. Kalarikkal, S. Thomas, Development of titanium dioxide nanowire incorporated poly(vinylidene fluoride–trifluoroethylene) scaffolds for bone tissue engineering applications, J. Mater. Sci. Mater. Med. 30 (2019) 96, https://doi.org/10.1007/s10856-019-6300-4.
[53] R. Augustine, Y.B. Dalvi, V.K. Yadu Nath, R. Varghese, V. Raghuveeran, A. Hasan, S. Thomas, N. Sandhyarani, Yttrium oxide nanoparticle loaded scaffolds with enhanced cell adhesion and vascularization for tissue engineering applications, Mater. Sci. Eng. C. 103 (2019) 109801, https://doi.org/10.1016/j.msec.2019.109801.
[54] R. Augustine, Y.B. Dalvi, P. Dan, N. George, D. Helle, R. Varghese, S. Thomas, P. Menu, N. Sandhyarani, Nanoceria can act as the cues for angiogenesis in tissue-engineering scaffolds: toward next-generation in situ tissue engineering, ACS Biomater. Sci. Eng. 4 (2018) 4338–4353, https://doi.org/10.1021/acsbiomaterials.8b01102.
[55] Z. Rezvani, J.R. Venugopal, A.M. Urbanska, D.K. Mills, S. Ramakrishna, M. Mozafari, A bird's eye view on the use of electrospun nanofibrous scaffolds for bone tissue engineering: current state-of-the-art, emerging directions and future trends, Nanomedicine nanotechnology, Biol. Med. 12 (2016) 2181–2200, https://doi.org/10.1016/j.nano.2016.05.014.
[56] N. Johari, M. Fathi, Z. Fereshteh, S. Kargozar, A. Samadikuchaksaraei, The electrospun poly(ε-caprolactone)/fluoridated hydroxyapatite nanocomposite for bone tissue engineering, Polym. Adv. Technol. 31 (2020) 1019–1026, https://doi.org/10.1002/pat.4836.
[57] S. Nazarnezhad, F. Baino, H.W. Kim, T.J. Webster, S. Kargozar, Electrospun nanofibers for improved angiogenesis: promises for tissue engineering applications, Nanomaterials. 10 (2020) 1–35, https://doi.org/10.3390/nano10081609.
[58] Z.-M.M. Huang, Y.-Z.Z. Zhang, M. Kotaki, S. Ramakrishna, A review on polymer nanofibers by electrospinning and their applications in nanocomposites, Compos. Sci. Technol. 63 (2003) 2223–2253, https://doi.org/10.1016/S0266-3538(03)00178-7.
[59] R. Augustine, S.K. Nethi, N. Kalarikkal, S. Thomas, C.R. Patra, Electrospun polycaprolactone (PCL) scaffolds embedded with europium hydroxide nanorods (EHNs) with enhanced vascularization and cell proliferation for tissue engineering applications, J. Mater. Chem. B 5 (2017) 4660–4672, https://doi.org/10.1039/c7tb00518k.
[60] R. Augustine, N. Kalarikkal, S. Thomas, An in vitro method for the determination of microbial barrier property (MBP) of porous polymeric membranes for skin substitute and wound dressing applications, Tissue Eng. Regen. Med. 12 (2014) 12–19, https://doi.org/10.1007/s13770-014-0032-9.
[61] A.I. Van Den Bulcke, B. Bogdanov, N. De Rooze, E.H. Schacht, M. Cornelissen, H. Berghmans, Structural and rheological properties of methacrylamide modified gelatin hydrogels, Biomacromolecules. 1 (2000) 31–38, https://doi.org/10.1021/bm990017d.
[62] R. Augustine, A. Hasan, V.K. Yadu Nath, J. Thomas, A. Augustine, N. Kalarikkal, A.E. Al Moustafa, S. Thomas, Electrospun polyvinyl alcohol membranes incorporated with green synthesized silver nanoparticles for wound dressing applications, J. Mater. Sci. Mater. Med. 29 (2018) 205–212, https://doi.org/10.1007/s10856-018-6169-7.
[63] R. Augustine, E.A. Dominic, I. Reju, B. Kaimal, N. Kalarikkal, S. Thomas, Investigation of angiogenesis and its mechanism using zinc oxide nanoparticle-loaded electrospun tissue engineering scaffolds, RSC Adv. 4 (2014) 51528–51536, https://doi.org/10.1039/c4ra07361d.
[64] D. Roman, A. Yasmeen, M. Mireuta, I. Stiharu, A.E. Al Moustafa, Significant toxic role for single-walled carbon nanotubes during normal embryogenesis, nanomedicine nanotechnology, Biol. Med. 9 (2013) 945–950, https://doi.org/10.1016/j.nano.2013.03.010.
[65] R. Augustine, P. Dan, A. Sosnik, N. Kalarikkal, N. Tran, B. Vincent, S. Thomas, P. Menu, D. Rouxel, Electrospun poly(vinylidene fluoride-trifluoroethylene)/zinc oxide nanocomposite tissue engineering scaffolds with enhanced cell adhesion and blood vessel formation, Nano Res. 10 (2017) 3358–3376, https://doi.org/10.1007/s12274-017-1549-8.
[66] R. Naphade, J. Jog, Electrospinning of PHBV/ZnO membranes: structure and properties, Fibers Polym. 13 (2012) 692–697, https://doi.org/10.1007/s12221-012-0692-9.
[67] Y. Zuo, X. Liu, D. Wei, J. Sun, W. Xiao, H. Zhao, L. Guo, Q. Wei, H. Fan, X. Zhang, Photo-cross-linkable methacrylated gelatin and hydroxyapatite hybrid hydrogel for modularly engineering biomimetic osteon, ACS Appl. Mater. Interfaces 7 (2015) 10386–10394, https://doi.org/10.1021/acsami.5b01433.
[68] R. Augustine, N. Kalarikkal, S. Thomas, Effect of zinc oxide nanoparticles on the *in vitro* degradation of electrospun polycaprolactone membranes in simulated body fluid, Int. J. Polym. Mater. Polym. Biomater. 65 (2016) 28–37, https://doi.org/10.1080/00914037.2015.1055628.
[69] L. Zhou, G. Tan, Y. Tan, H. Wang, J. Liao, C. Ning, Biomimetic mineralization of anionic gelatin hydrogels: effect of degree of methacrylation, RSC Adv. 4 (2014) 21997–22008, https://doi.org/10.1039/c4ra02271h.
[70] C.-C. Liang, A.Y. Park, J.-L. Guan, In vitro scratch assay: a convenient and inexpensive method for analysis of cell migration in vitro, Nat. Protoc. 2 (2007) 329–333, https://doi.org/10.1038/nprot.2007.30.
[71] A.D. Metcalfe, M.W.J.J. Ferguson, Tissue engineering of replacement skin : the crossroads of biomaterials , wound healing , embryonic development , stem cells and regeneration, J. R. Soc. Interface 4 (2007) 413–437. doi:https://doi.org/10.1098/rsif.2006.0179.
[72] R. Dimatteo, N.J. Darling, T. Segura, In situ forming injectable hydrogels for drug delivery and wound repair, Adv. Drug Deliv. Rev. 127 (2018) 167–184, https://doi.org/10.1016/j.addr.2018.03.007.
[73] R. Augustine, P. Dan, I. Schlachet, D. Rouxel, P. Menu, A. Sosnik, Chitosan ascorbate hydrogel improves water uptake capacity and cell adhesion of electrospun poly(epsilon-caprolactone) membranes, Int. J. Pharm. 559 (2019) 420–426, https://doi.org/10.1016/j.ijpharm.2019.01.063.
[74] T. Tsuji, R.M. Lavker, A.M. Kligman, A new method for scanning electron microscopic visualization of dermal elastic fibres, J. Microsc. 115 (1979) 165–173, https://doi.org/10.1111/j.1365-2818.1979.tb00166.x.
[75] S.E.G. Fligiel, J. Varani, S.C. Datta, S. Kang, G.J. Fisher, J.J. Voorhees, Collagen degradation in aged/photodamaged skin in vivo and after exposure to matrix metalloproteinase-1 in vitro, J. Invest. Dermatol. 120 (2003) 842–848, https://doi.org/10.1046/j.1523-1747.2003.12148.x.
[76] C.R. Nuttelman, D.J. Mortisen, S.M. Henry, K.S. Anseth, Attachment of fibronectin to poly(vinyl alcohol) hydrogels promotes NIH3T3 cell adhesion, proliferation, and migration, J. Biomed. Mater. Res. 57 (2001) 217–223, https://doi.org/10.1002/1097-4636(200111)57:2<217::AID-JBM1161>3.0.CO;2-I.
[77] A. Assmann, A. Vegh, M. Ghasemi-Rad, S. Bagherifard, G. Cheng, E.S. Sani, G.U. Ruiz-Esparza, I. Noshadi, A.D. Lassaletta, S. Gangadharan, A. Tamayol, A. Khademhosseini, N. Annabi, A highly adhesive and naturally derived sealant, Biomaterials. 140 (2017) 115–127, https://doi.org/10.1016/j.biomaterials.2017.06.004.
[78] B. Saleh, H.K. Dhaliwal, R. Portillo-Lara, E. Shirzaei Sani, R. Abdi, M.M. Amiji, N. Annabi, Local immunomodulation using an adhesive hydrogel loaded with miRNA-laden nanoparticles promotes wound healing, Small. 15 (2019) 1902232, https://doi.org/10.1002/smll.201902232.
[79] K. Murakami, H. Aoki, S. Nakamura, S. ichiro Nakamura, M. Takikawa, M. Hanzawa, S. Kishimoto, H. Hattori, Y. Tanaka, T. Kiyosawa, Y. Sato, M. Ishihara, Hydrogel blends of chitin/chitosan, fucoidan and alginate as healing-impaired wound dressings, Biomaterials. 31 (2010) 83–90. doi:https://doi.org/10.1016/j.biomaterials.2009.09.031.
[80] K. Modaresifar, A. Hadjizadeh, H. Niknejad, Design and fabrication of GelMA/chitosan nanoparticles composite hydrogel for angiogenic growth factor delivery, Artif. Cells, Nanomedicine, Biotechnol. 46 (2018) 1799–1808, https://doi.org/10.1080/21691401.2017.1392970.
[81] Z. Ruszczak, Effect of collagen matrices on dermal wound healing, Adv. Drug Deliv. Rev. 55 (2003) 1595–1611, https://doi.org/10.1016/J.ADDR.2003.08.003.
[82] O. Jeon, D.W. Wolfson, E. Alsberg, In-situ formation of growth-factor-loaded coacervate microparticle-embedded hydrogels for directing encapsulated stem cell fate, Adv. Mater. 27 (2015) 2216–2223, https://doi.org/10.1002/adma.201405337.
[83] X. Tang, B. Liu, X. Wang, Q. Yu, R. Fang, Epidermal growth factor, through alleviating oxidative stress, protect IPEC-J2 cells from lipopolysaccharides-induced apoptosis, Int. J. Mol. Sci. 19 (2018) 848, https://doi.org/10.3390/ijms19030848.
[84] M. Rodrigues, H. Blair, L. Stockdale, L. Griffith, A. Wells, Surface tethered epidermal growth factor protects proliferating and differentiating multipotential stromal cells from FasL-induced apoptosis, Stem Cells 31 (2013) 104–116, https://doi.org/10.1002/stem.1215.
[85] Y.J. Son, J.W. Tse, Y. Zhou, W. Mao, E.K.F. Yim, H.S. Yoo, Biomaterials and controlled release strategy for epithelial wound healing, Biomater. Sci. 7 (2019) 4444–4471, https://doi.org/10.1039/c9bm00456d.
[86] J.C. Cheng, N. Auersperg, P.C.K. Leung, EGF-induced EMT and invasiveness in serous borderline ovarian tumor cells: a possible step in the transition to low-grade serous carcinoma cells? PLoS One 7 (2012) e34071, , https://doi.org/10.1371/

journal.pone.0034071.
[87] J.T. Kim, E.H. Lee, K.H. Chung, I.C. Kang, D.H. Lee, C.K. Joo, Transdifferentiation of cultured bovine lens epithelial cells into myofibroblast-like cells by serum modulation, Yonsei Med. J. 45 (2004) 380–391, https://doi.org/10.3349/ymj.2004.45.3.380.
[88] D. Kim, S.Y. Kim, S.K. Mun, S. Rhee, B.J. Kim, Epidermal growth factor improves the migration and contractility of aged fibroblasts cultured on 3D collagen matrices, Int. J. Mol. Med. 35 (2015) 1017–1025, https://doi.org/10.3892/ijmm.2015.2088.
[89] C.L. Chaffer, B.P. San Juan, E. Lim, R.A. Weinberg, EMT, cell plasticity and metastasis, Cancer Metastasis Rev. 35 (2016) 645–654, https://doi.org/10.1007/s10555-016-9648-7.
[90] L.S. Royce, B.J. Baum, Physiologic levels of salivary epidermal growth factor stimulate migration of an oral epithelial cell line, BBA - Mol. Cell Res. 1092 (1991) 401–403, https://doi.org/10.1016/S0167-4889(97)90019-7.
[91] J. Feng, G.E. Besner, Heparin-binding epidermal growth factor-like growth factor promotes enterocyte migration and proliferation in neonatal rats with necrotizing enterocolitis, J. Pediatr. Surg. 42 (2007) 214–220, https://doi.org/10.1016/j.jpedsurg.2006.09.055.
[92] Y. Shirakata, R. Kimura, D. Nanba, R. Iwamoto, S. Tokumaru, C. Morimoto, K. Yokota, M. Nakamura, K. Sayama, E. Mekada, S. Higashiyama, K. Hashimoto, Heparin-binding EGF-like growth factor accelerates keratinocyte migration and skin wound healing, J. Cell Sci. 118 (2005) 2363–2370, https://doi.org/10.1242/jcs.02346.
[93] J.D. Chen, J.P. Kim, K. Zhang, Y. Sarret, K.C. Wynn, R.H. Kramer, D.T. Woodley, Epidermal growth factor (EGF) promotes human keratinocyte locomotion on collagen by increasing the α2 integrin subunit, Exp. Cell Res. 209 (1993) 216–223, https://doi.org/10.1006/excr.1993.1304.
[94] G.R. Grotendorst, Y. Soma, K. Takehara, M. Charette, EGF and TGF-alpha are potent chemoattractants for endothelial cells and EGF-like peptides are present at sites of tissue regeneration, J. Cell. Physiol. 139 (1989) 617–623, https://doi.org/10.1002/jcp.1041390323.
[95] M. Mawatari, K. Okamura, T. Matsuda, R. Hamanaka, H. Mizoguchi, K. Higashio, K. Kohno, M. Kuwano, Tumor necrosis factor and epidermal growth factor modulate migration of human microvascular endothelial cells and production of tissue-type plasminogen activator and its inhibitor, Exp. Cell Res. 192 (1991) 574–580, https://doi.org/10.1016/0014-4827(91)90078-9.
[96] G. Livshits, A. Kobielak, E. Fuchs, Governing epidermal homeostasis by coupling cell-cell adhesion to integrin and growth factor signaling, proliferation, and apoptosis, Proc. Natl. Acad. Sci. 109 (2012) 4886–4891, https://doi.org/10.1073/pnas.1202120109.
[97] S. Guo, L. a Dipietro, factors affecting wound healing, J. Dent. Res. 89 (2010) 219–229, https://doi.org/10.1177/0022034509359125.
[98] P.P. Ongusaha, J.C. Kwak, A.J. Zwible, S. Macip, S. Higashiyama, N. Taniguchi, L. Fang, S.W. Lee, HB-EGF is a potent inducer of tumor growth and angiogenesis, Cancer Res. 64 (2004) 5283–5290, https://doi.org/10.1158/0008-5472.CAN-04-0925.
[99] K.P. Koster, R. Thomas, A.W.J. Morris, L.M. Tai, Epidermal growth factor prevents oligomeric amyloid-β induced angiogenesis deficits in vitro, J. Cereb. Blood Flow Metab. 36 (2016) 1865–1871, https://doi.org/10.1177/0271678X16669956.
[100] S.B. Catrina, X. Zheng, Disturbed hypoxic responses as a pathogenic mechanism of diabetic foot ulcers, Diabetes Metab. Res. Rev. 32 (2016) 179–185, https://doi.org/10.1002/dmrr.2742.
[101] Y.S. Kim, D.K. Sung, W.H. Kong, H. Kim, S.K. Hahn, Synergistic effects of hyaluronate-epidermal growth factor conjugate patch on chronic wound healing, Biomater. Sci. 6 (2018) 1020–1030, https://doi.org/10.1039/c8bm00079d.
[102] J. Xu, D. Min, G. Guo, X. Liao, Z. Fu, Experimental study of epidermal growth factor and acidic fibroblast growth factor in the treatment of diabetic foot wounds, Exp. Ther. Med. 15 (2018) 5365–5370, https://doi.org/10.3892/etm.2018.6131.
[103] P.B. Milan, N. Lotfibakhshaiesh, M.T. Joghataie, J. Ai, A. Pazouki, D.L. Kaplan, S. Kargozar, N. Amini, M.R. Hamblin, M. Mozafari, A. Samadikuchaksaraei, Accelerated wound healing in a diabetic rat model using decellularized dermal matrix and human umbilical cord perivascular cells, Acta Biomater. 45 (2016) 234–246, https://doi.org/10.1016/j.actbio.2016.08.053.
[104] Q. Shi, Z. Qian, D. Liu, J. Sun, X. Wang, H. Liu, J. Xu, X. Guo, GMSC-derived exosomes combined with a chitosan/silk hydrogel sponge accelerates wound healing in a diabetic rat skin defect model, Front. Physiol. 8 (2017). doi:https://doi.org/10.3389/fphys.2017.00904.